

UNDRAINED CYCLIC SHEAR BEHAVIOR OF CLAY UNDER DRASTICALLY CHANGED LOADING RATE

*Imran Khan¹, Kentaro Nakai² and Toshihiro Noda³

^{1,2}Faculty of Engineering, Nagoya University, Japan; ³ Mitigation Research Center, Nagoya University, Japan

*Corresponding Author, Received: 30 Oct. 2019, Revised: 22 Nov. 2019, Accepted: 01 Jan. 2020

ABSTRACT: The earthquake damage prediction is mainly focused on the seismic instability of sandy foundations although the clayey foundation could also be vulnerable to earthquake damage. Moreover, it is known that clayey soil shows a marked loading rate dependency in monotonic shear behavior due to its low permeability. Therefore, this paper aims to determine the undrained cyclic shear behavior of clayey soil under a drastically changed loading rate. Reconstituted clayey samples were subjected to undrained cyclic triaxial compression/extension tests with loading rate from 1.0Hz to 0.0042Hz by stress control, and 0.01%/min by strain control. The cyclic loading was stopped when the double amplitude exceeded 5%. Then, the specimen was left for a while in an undrained condition, until the value of pore water pressure converged. Results revealed that as the loading rate decreases, the number of cycles that corresponds to DA=2% and 5% also decreased. Therefore, the degree of strain evolution varies depending on the loading rate and the undrained shear strength also varies depending on the cyclic loading rate. This is because when the cyclic loading rate was high; the pore water did not migrate sufficiently, leading to the non-uniform distribution of the excess pore water pressure inside the specimen. However, the final values of excess pore water pressure after the homogenization process was the same regardless of the loading rate. This means that if sufficient time is left after cyclic loading, the final mean effective stress value becomes equal regardless of the loading rate.

Keywords: Clay, Cyclic loading, Loading rate, Excess pore water pressure

1. INTRODUCTION

Since the liquefaction damage to sandy soils has been noticed by the Niigata Earthquake in 1964 and the Alaska Earthquake in 1964, the earthquake damage prediction of the ground / soil structure has been mainly focused on the seismic instability of the sandy foundations. On the other hand, even if the clayey soil which has an N-value of zero or contains a large amount of sand / silt, as soon as it is classified as "clay", it has been often considered that earthquake damage does not occur and it has been virtually modeled as an elastic material in the past. However, in fact, it is not the case that earthquake damage has not really occurred on clayey foundations. If the past earthquake damage is examined carefully, although there are not many cases like liquefaction damage of sandy foundation, earthquake damage of clayey foundation can be also observed.

It is known that the damage to the clayey foundation at the time of the Mexico City earthquake in 1985 caused tremendous human and structural damage in Mexico City far from the epicenter. Mexico City is located on the ground made by reclaiming of old Texcoco Lake, and soft volcanic ashy clay was deposited thickly. This soft clay lost its bearing capacity during the earthquake, causing overturning damage to structures [1,2]. In

addition to the structural damage during the earthquake, the settlement of the clay layer accelerated immediately after the earthquake, and continued for a long time [3].

Similar earthquake damage, thought to be caused mainly by clayey soil, has also been observed both in Japan and abroad. Long-term continuous settlement damage of the Niigata plain by the off the coast of Miyagi earthquake in 1978 [4] and Chuetsu earthquake in 2007 [5], settlement acceleration of Port Island by the 1995 Southern Hyogo Prefecture Earthquake [6]. In recent years, collapse of soil structures in the Kathmandu Valley caused by the Nepal earthquake in 2015, and Graben-like cracks in the Aso caldera caused by the Kumamoto earthquake in 2016 could be also considered to be earthquake damage of clayey material.

Laboratory tests on the dynamic properties of clayey soil have been conducted since earthquake damage of clayey foundation began to be noticed. In general, it is known that clayey soil shows a marked loading rate dependency in monotonic shear behavior due to its low permeability [7-11]. Also, in order to overcome such a problem as non-uniformity of pore water pressure distribution inside the specimen and to treat the experimental results as "element behavior," it is common to apply load as slowly as possible for static loading

test. Therefore, in order to investigate the undrained cyclic shear characteristics of clayey soil, it is necessary to evaluate the effect of loading rate in mind [12-17]. However, the range of the loading rate of the cyclic loading test that has been performed so far is narrower than that of the static loading test. Furthermore, many of the experiments so far have focused on the cyclic shear strength during cyclic loading, but few experiments have been conducted to observe in detail, the dissipation process of excess pore water pressure after cyclic loading that became non-uniform during cyclic loading.

As a basic experiment of clayey material, the purpose of this paper is to understand the undrained cyclic shear behavior of clayey soil under a drastically changed loading rate. Since clay material has low permeability, there is a difference in excess pore water pressure migration depending on the loading rate. Especially when the loading rate is high, the pore water does not migrate sufficiently during cyclic loading and the excess pore water pressure distribution inside the specimen becomes non-uniform. Therefore, the specimen was left for a while in an undrained condition after cyclic loading, until the excess pore water pressure distribution inside the specimen became uniform.

2. PHYSICAL PROPERTIES OF SAMPLE USED IN THE EXPERIMENT

Figure 1 shows the grain size distribution and Table 1 shows the physical properties of the sample used in the experiment respectively. Over 90% is occupied by fine particles (silt / clay), and it is classified as “CL” (low liquid limit clayey

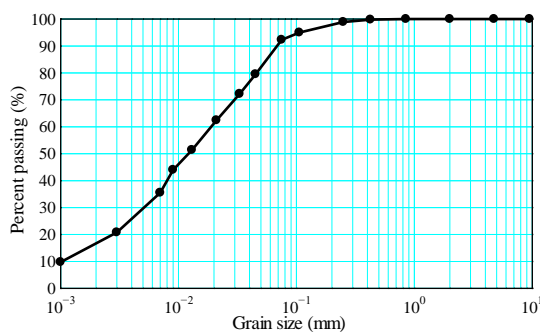


Fig.1 Grain size distribution

Table 1 Physical properties of the sample

Soil particle density ρ_s (g/cm ³)	2.69
Liquid limit w_L (%)	45.8
Plastic limit w_p (%)	25.3
Plasticity index I_p	20.5

soil) by Japanese classification of geomaterials [18]. The water content of the slurry-like sample, was adjusted to twice the liquid limit ($w=90\%$), and the sample was thoroughly stirred and degassed. Then, it was placed in a pre-consolidation tank, and one-dimensional consolidation was performed at a vertical stress of 200kPa for one week to prepare a reconstituted sample.

3. MONOTONIC SHEAR BEHAVIOR WITH DIFFERENT LOADING RATE

Monotonic drained and undrained triaxial compression tests under various constant axial strain rates were conducted. Confining pressure was set to 300kPa (back pressure 200kPa, lateral pressure 500kPa) so that normal consolidated state could be achieved for all specimens. All the experimental results shown below had a B-value of 0.95 or higher. Figure 2 shows the results of drained triaxial compression tests conducted at various loading rates. The lower the axial strain rate, the greater the failure or maximum shear strength. In Case-[4], the loading rate of which was the highest, there was almost no volumetric change during shearing, even though the test was conducted under drainage conditions. As the loading rate became lower, volumetric change during shearing tended to occur. Therefore, the shear strength increased as the loading rate decreased. Figure 3 shows the results of undrained triaxial compression tests conducted at various loading rates. Contrary to drained shear behavior, a higher the axial strain rate correspond to a, greater failure or maximum shear strength. This is due to the migration of pore water. Because excess pore water pressure was generated non-uniformly inside the specimen along with shearing, a gradient occurred in the water pressure, and pore water migration occurred inside the specimen even though the total volume was constant [19]. If the loading rate is high and the excess pore water pressure distribution is more non-uniform, the water pressure gradient becomes larger, and pore water migration is likely to occur. However, in Case-[4], because the loading rate is high, there would be almost no migration of pore water, and the specific volume would remain in a uniform state. On the other hand, when the loading rate is low, pore water migration occurs, and thus the specific volume becomes non-uniform inside the specimen. Since the specific volume of the entire specimen did not change under undrained conditions, the shear strength became stronger when the specific volume was uniform. Furthermore, it can be seen that mean effective stress p' increased in the effective stress path at the initial stage of loading as the axial strain rate

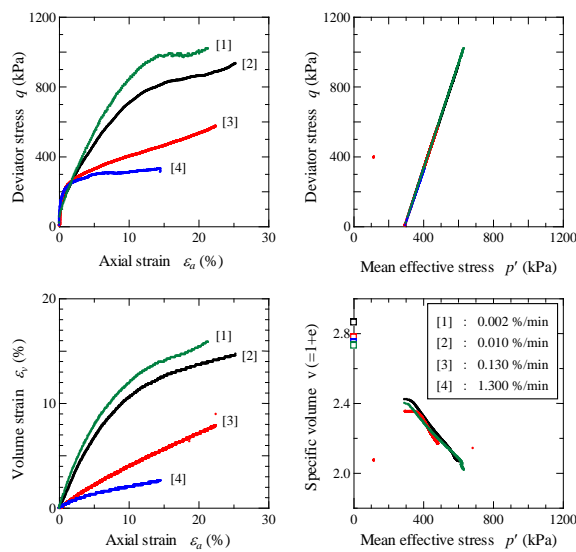


Fig.2 Drained triaxial compression tests with different loading rate

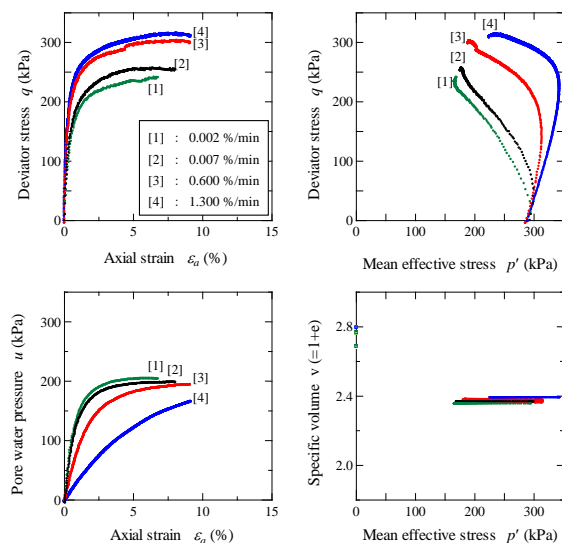


Fig.3 Undrained triaxial compression tests with different loading rate

increases. In particular, at the most rapid loading rate (Case-[4]), the effective stress path almost coincided with the total stress path ($q/p'=3$). If the axial strain rate was sufficiently low, the pore water pressure distributed uniformly. However, when the axial strain rate was high, the pore water pressure accumulated in the center of the specimen and was unlikely to occur at both ends. Because pore water pressure was measured at the lower end of the specimen, the pore water pressure could not be measured accurately or be measured smaller value when the axial strain rate is higher. As a result, p' at the beginning of loading became larger.

Figure 4 shows a summary of the loading rate effect. The drained shear tests draw an inverted S-

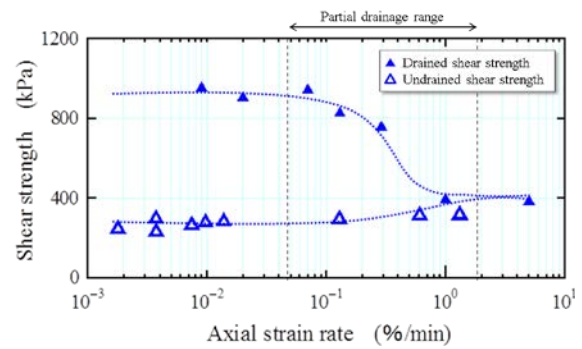


Fig.4 Shear strength with different drainage condition and loading rate

shaped curve, and the undrained shear tests draw an S-shaped curve, and the drained shear strength is greater than the undrained one. At a high loading rate of 1.0×10^0 %/min or higher, pore water migration does not occur, so the shear strength matches regardless of drainage conditions. However, if the loading rate is 1.0×10^{-2} %/min or less, pore water migration sufficiently occurs, and neither drained nor undrained shear strength changes any more. When the loading rate is between these values, the shear strength changes due to the partial drainage effect accompanying the migration of pore water.

Nakano [11] focused on the experimental fact that the loading rate range in which drained and undrained shear strength changed were almost equal, and one of the causes of the loading rate effect was that the specimen was non-uniform due to the difference in pore water migration. Asaoka and Noda [20] found that mode-switching occurred due to the migration of excess pore water which resulted in the difference of drained and undrained shear strength through the numerical analyses. Thus, it has been shown both experimentally and numerically that the non-uniformity of excess pore water pressure distribution caused by differences in loading rates has a great influence on the shear strength.

4. UNDRAINED CYCLIC SHEAR BEHAVIOR WITH DIFFERENT LOADING RATE

Many experiments have been conducted to understand the dynamic properties of clayey soil. In order to understand the effect of loading rate on undrained cyclic shear behavior, undrained cyclic triaxial compression/extension tests were conducted under constant stress amplitude conditions. Confining pressure was set to 300kPa (back pressure 200kPa, lateral pressure 500kPa) so that a normal consolidation state could be achieved. All the experimental results shown below had a B-value of 0.95 or higher. Stress amplitude was

given by 120kPa (stress amplitude ratio = 0.4). Loading conditions are shown in Tables 2 and 3. Cases -A to E were performed by stress control with a sinusoidal waveform changing the loading rate from 1.0×10^0 Hz to 4.2×10^{-4} Hz. Case-F was carried out by strain control with a constant rate 1.0×10^{-2} %/min, which is considered to be low enough that the pore water migration occurs sufficiently. In all cases, cyclic loading was stopped when DA (double amplitude) exceeded 5%. Then, the specimen was left for a while in an undrained condition after cyclic loading, until the value of pore water pressure (mean effective stress p') converged.

Table 2 Loading rate under stress control

Case	Loading rate	
	Frequency	Period (s)
A	1.0×10^0	1
B	1.0×10^{-1}	10
C	5.0×10^{-2}	20
D	1.7×10^{-3}	600
E	4.2×10^{-4}	2400

Table 3 Loading condition under strain control

Case	Loading rate (%/min)
F	1.0×10^{-2}

4.1 Undrained Cyclic Shear Behavior

First, shear behavior during cyclic loading is described. Experimental results (stress ~ strain curves and stress paths) are shown in Figures 5 to 10. Mean effective stress is calculated using the pore water pressure measured at the lower end of the specimen as a representative value.

In Case-A, the loading rate of which is high, the p' hardly decreased (excess pore water pressure was hardly measured) during cyclic loading. Moreover, the effective stress path almost coincided with the total stress path ($q/p'=3$). As mentioned in section 3, excess pore water pressure measured at the lower end of the specimen decreased when the axial strain rate was high. Similar to the change of effective stress, axial strain was also hardly generated at the initial stage of repetition, but the strain progressed gradually as repetition continued. In Case-B, the loading rate of which is 10 times lower than Case-A, decrease of p' became obvious compared with Case-A. Mean effective stress tended to decrease relatively early in the initial repetition and eventually converged. Axial strain was also more likely to occur than in Case-A, but the tendency for strain to be small during the initial stage of loading and gradually

increase was the same. It can be seen that as the loading rate decreased from Case-B to Case-E, the p' decreased more with the repetition and axial strain also tended to be generated at the same time. In Case-F, which loaded slowly enough to cause sufficient pore water migration, showed the largest decrease of p' at the initial loading stage compared with other conditions. Furthermore, axial strain also increased from the beginning of the loading.

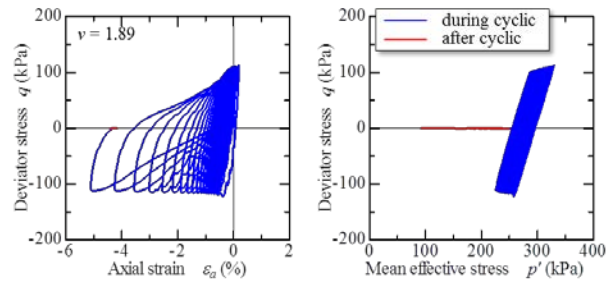


Fig.5 Case-A (stress control with 1.0×10^0 Hz)

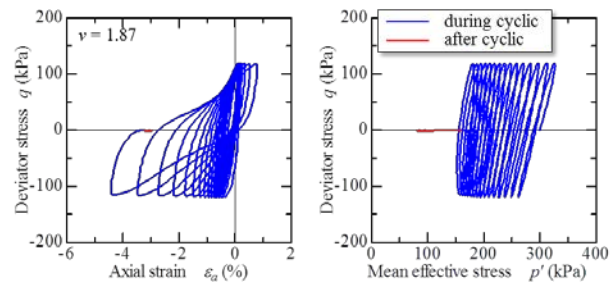


Fig.6 Case-B (stress control with 1.0×10^{-1} Hz)

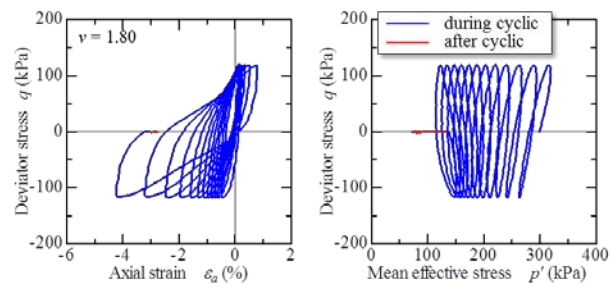


Fig.7 Case-C (stress control with 5.0×10^{-2} Hz)

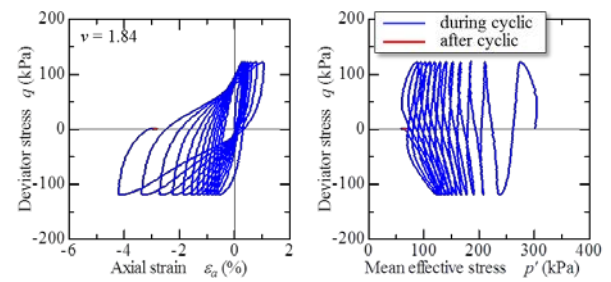


Fig.8 Case-D (stress control with 1.7×10^{-3} Hz)

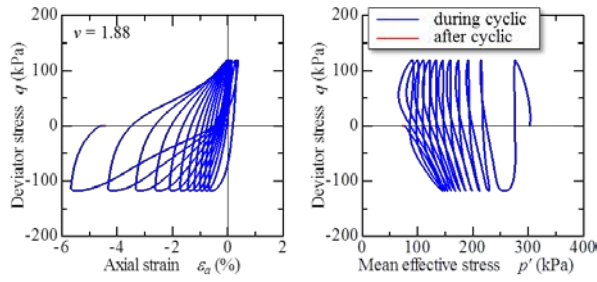


Fig.9 Case-E (stress control with 4.2×10^{-4} Hz)

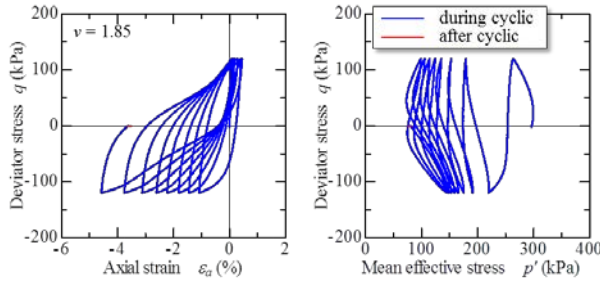


Fig.10 Case-F (strain control with 1.0×10^{-2} %/min)

Figure 11 shows the relationship between the number of cycles and the progress of maximum / minimum axial strain. Axial strain was unlikely to occur at the beginning of cycles, but when the number of cycles increased to some extent, the axial strain progressed at an accelerated rate. In addition, the higher the loading rate, the more strain began to generate even if the number of cycle is small. The strain progress was more pronounced on the extension side than on compression side. This is due to the anisotropy effect which was developed during the pre-consolidation process. Because the pre-consolidation load was applied in the vertical direction, the specimen might be more resistant/stronger to compression side than the expansion side. Table 4 shows the number of cycle when DA reached 2% and 5%. As the loading rate became lower, the number of cycles that

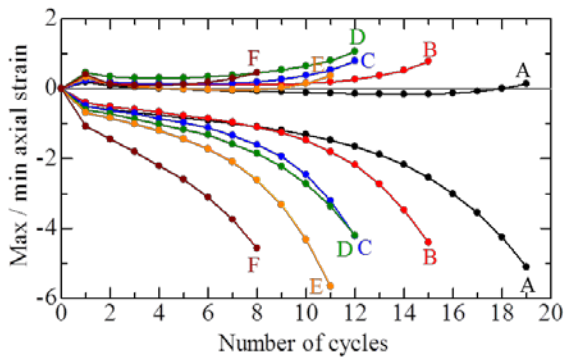


Fig.11 Progress of axial strain with increasing cycles

Table 4 Number of cycle until predetermined DA

Case	Number of cycle	
	DA=2%	DA=5%
A	14	19
B	11	15
C	9	12
D	8	12
E	7	11
F	4	8

corresponds to DA=2% and 5% clearly decreased. Undrained cyclic shear strength is often evaluated by the number of cycles to reach a given DA. It can be seen that the undrained cyclic shear strength varied greatly depending on the loading rate, and that the cyclic shear strength decreased as the loading rate became lower.

4.2 Excess Pore Water Pressure Uniformity Process after Cyclic Loading

Next, uniformity process in excess pore water pressure after cyclic loading are examined. Figure 12 shows the relationship between the number of cycles and the excess pore water pressure (measured at the bottom end of the specimen).

Case-A, which has the most rapid loading rate, generated small excess pore water pressure during cyclic loading. As the loading rate became lower, the excess pore pressure increased with ongoing repetition. Figure 12 also shows the change in excess pore water pressure after stopping cyclic loading (denoted by filled circle marks), while maintaining the undrained condition. In Case-A, excess pore water pressure increased greatly after cyclic loading. The lower the cyclic loading rate, the less the excess pore water pressure rose after cyclic loading, and there was almost no change after Case-D. As mentioned in section 3., when the cyclic loading rate was high, the excess pore water

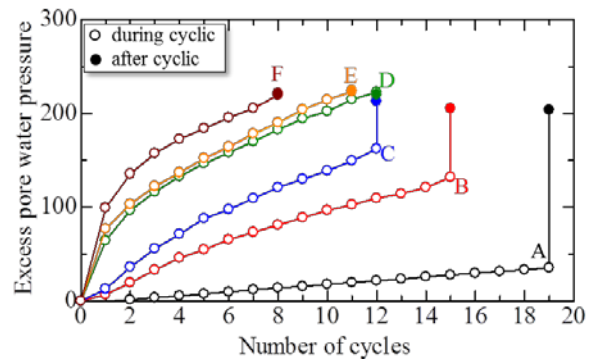


Fig.12 Excess pore water pressure change with increasing cycles

pressure distribution inside the specimen became non-uniform during shearing. The increase of excess pore water pressure was measured in the process of uniforming the excess pore water pressure distribution after cyclic loading. In all experimental results from Cases A to F, cyclic loading was stopped at DA=5%. Considering the uniformity process of the excess pore water pressure, the final value of excess pore water pressure seems to be the same in all cases or slightly larger if the loading rate is lower. This means that if sufficient time is left after cyclic loading, the final mean effective stress value becomes equal regardless of the loading rate.

5. COMPRESSION BEHAVIOR AFTER CYCLIC LOADING

Excess pore water pressure accumulated by undrained cyclic loading will dissipate and show consolidation when the specimen is changed to a drained condition. Until now, attempts have been made to understand the compression behavior of clayey soil subjected to cyclic loading, and the relationship with the compression index or swelling index has been studied [13,21-23]. Therefore, after the excess pore water pressure change ceased after cyclic loading, the drainage valve was opened while maintaining isotropic stress condition and the volume change of the specimen was measured.

Table 5 shows the slopes of the compression lines obtained through the reconsolidation process. The slopes were calculated from two points: before and after opening the valve. Regardless of the cyclic loading rate, the values of the recompression gradient were the same, and the average value is 0.04. Figure 13 shows experimental results from a standard consolidation test using reconstituted specimens. Compression index C_c and swelling index C_s obtained from the results were 0.590 and 0.020 respectively. The slopes of the compression line after cyclic loading was smaller than the compression index C_c and was equal to or slightly larger than the swelling index C_s . This means that the amount of compression after cyclic loading

Table 5 Slopes of compression line obtained through reconsolidation process

Case	Recompression gradient
A	0.043
B	0.041
C	0.034
D	0.044
E	0.040
F	0.044

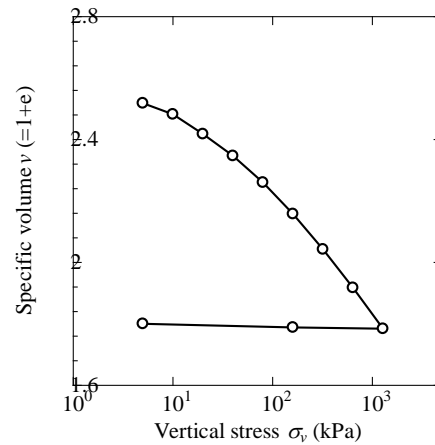


Fig.13 Standard consolidation test

would be determined based on the swelling index. However, there might be a risk of underestimating the amount of compression unless the decrease in p' due to uniformity

6. DISCUSSION AND CONCLUSION

This paper shows the results of undrained cyclic triaxial compression/extension tests of reconstituted clay specimens with different loading rates, which were conducted as basic experiments for grasping the dynamic characteristics of clayey materials. The loading rate was changed drastically from 1.0Hz to 0.0042Hz by stress control, and 0.01%/min by strain control which was considered to be low enough that pore water migration occurs sufficiently during shearing. Moreover, observation of the uniformity process of excess pore water pressure after cyclic loading, and a re-compression test after cyclic loading were also conducted. The following results were obtained from the experimental results.

- (1) The degree of strain evolution varied depending on the loading rate. Because undrained shear strength is often evaluated by the number of cycles to reach a given DA (double amplitude), this experimental fact indicates that the undrained shear strength also varies depending on the cyclic loading rate. The lower the loading rate is, the weaker the strength becomes.
- (2) In the triaxial test apparatus, mean effective stress p' is calculated using the excess pore pressure measured at the lower end of the specimen as a representative value. When the cyclic loading rate is high, the pore water does not migrate sufficiently and the distribution of the excess pore water pressure inside the specimen becomes non-uniform (the measured value of the excess pore water pressure becomes small). Therefore, the (apparent) effective stress path varies depending on the loading rate. When the loading rate is high,

the effective stress path hardly decreases during the repetition.

- (3) During the uniformity process after cyclic loading, the measured value of excess pore water pressure at the end of the specimen increased (mean effective stress decrease). Higher the cyclic loading rates generated, greater excess pore water pressure. However, the final values of excess pore water pressure after the homogenization process was the same regardless of loading rate or slightly larger if the loading rate was lower. This means that if sufficient time is left after cyclic loading, the final mean effective stress value becomes equal regardless of the loading rate.
- (4) Slopes of compression lines after cyclic loading were equal regardless of the cyclic loading rate and this value was smaller than the compression index C_c , and equal to or slightly larger than the swelling index C_s . This means that the amount of compression after cyclic loading would be determined based on the swelling index. However, there might be a risk of underestimating the amount of compression unless the decrease in p' due to uniformity process of excess pore water pressure is taken into account.

There are various types of external cyclic forces, such as earthquake motion, coastal waves, and traffic loads, which are actual problems. These all have different loading cycles from rapid loading to slow loading. Since the cyclic shear strength varies depending on the loading rate, it is important to conduct experiments using a suitable loading rate compared with the target problem. In other words, it is important to treat as an initial boundary value problem. In the development of a constitutive equation, it is important to grasp the element characteristics of the material accurately. Therefore, it is important to obtain experimental results at the lowest possible loading rate so that the internal state of the specimen can be treated as homogeneous and uniform. In this paper, reconstructed samples were used, but experiments using undisturbed samples from the naturally deposited condition will be conducted in the future to understand the effects of soil skeletal structure and its disturbance.

7. REFERENCES

- [1] J. Merlos and M. P. Romo, Fluctuant bearing capacity of shallow foundations during earthquakes, *Soil Dynamics and Earthquake Engineering*, No.26, 2006, pp.103-114.
- [2] Mendoza, M. J., Foundation engineering in Mexico City; Behavior of foundations, *Proceeding of International Symposium on Geotechnical Engineering of Soft Clay*, Vol.2, 1987, pp.351-367.
- [3] Leonardo Zeevaert., *Foundation Engineering for Difficult Subsoil Conditions*, Van Nostrand Reinhold Company, 1972, pp. 521.
- [4] Towhata, I., *Geotechnical Earthquake Engineering*, Springer, 2008, pp.359.
- [5] Isobe, K., Ohtsuka, S. and Takahara, T., Study on long-term subsidence of soft clay due to 2007 Niigata Prefecture Chuetsu-Oki Earthquake, *Proceedings of 18th ICSMGE*, 2013, pp.1499-1502.
- [6] Matsuda, H. and Nagira, H., Decrease in effective stress and reconsolidation of saturated clay induced by cyclic shear, *Journal of JSCE*, No. 659, III-52, 2000, pp. 63-75.
- [7] Skempton, A. W. and Bishop, A. W., *Soils*, Chapter X of *Building Materials*, North Holland Publ. Co., Amsterdam, 1954, pp.417-482.
- [8] Vaid, Y. P. and Campanella, R. G., Time-dependent behavior of an undisturbed clay, *The University of British Columbia Soil Mechanics Series*, No.33, 1977.
- [9] Sekiguchi, H., Nishida, Y. and Kanai, F., Analysis of partially-drained triaxial testing of clay, *Soils and Foundations*, Vol.21, No.3, 1981, pp.53-66.
- [10] Tonosaki, A., Akaishi, M., Saitoh, H. and Inada, M., Effects of loading speed and dilatancy of saturated clays, *Soils and Foundations*, Vol.27, No.4, 1987, pp.200-203, in Japanese.
- [11] Nakano, M., Analysis of undrained and partially drained shear behavior of clay and its application to embankment design on soft ground, *Doctoral Dissertation*, Nagoya University, 1993, in Japanese.
- [12] Procter, D. C. and Khaffaf, J. H., Cyclic triaxial tests on remoulded clays, *Journal of Geotechnical Engineering*, ASCE, Vol.110, No.10, 1984, pp.1431-1445.
- [13] Matsui, T., Ohara, H. and Ito, T., Effects of dynamic stress history on mechanical characteristics of saturated clays, *Journal of JSCE*, No.257, 1977, pp.41-51, in Japanese.
- [14] Yasuhara, K., Yamanouchi, T. and Hirao, K., Cyclic strength and deformation of normally consolidated clay, *Soils and Foundations*, Vol.22, No.3, 1982, pp. 77-91.
- [15] Hyodo, M., Shinomiya, K., Yasufuku, N. and Murata, S., Cyclic strengths of clay and sand by strain rate controlled cyclic triaxial test, *Journal of JSCE*, No.523, III-32, 1995, pp.9-18, in Japanese.
- [16] Yamamoto, Y. and Hyodo, M., The rate effect of cyclic shear characteristics of clays, *Journal of JSCE*, No.645, III-50, 2000, pp.63-76, in Japanese.

- [17] Byung-Woong Song., Yasuhara, K. and Murakami, S., An estimating method for post-cyclic strength and stiffness of fine-grained soils in direct simple shear tests, *Journal of the Korean Geotechnical Society*, Vol.20, No.2, 2004, pp.15-26.
- [18] The Japanese Geotechnical Society, *Japanese Geotechnical Society Standards – Laboratory testing standards of Geomaterials –*, 2015.
- [19] Asaoka, A., Nakano, M. and Noda, T., Soil-water coupled behavior of saturated clay near/at critical state, *Soils and Foundations*, Vol.34, No.1, 1994, pp.91-105.
- [20] Asaoka, A. and Noda, T. (1995): Imperfection-sensitive bifurcation of Cam-clay under plane strain compression with undrained boundaries, *Soils and Foundations*, Vol.35, No.1, pp.83-100.
- [21] Suzuki, T., Settlement of saturated clays under dynamic stress history, *Journal of the Japan Society of Engineering Geology*, Vol.25, No.3, 1984, pp.21-31, in Japanese.
- [22] Yasuhara, K. and Andersen, K. H., Recompression of normally consolidated clay after cyclic loading, *Soils and Foundations*, Vol.31, No.1, 1991, pp.83-94.
- [23] O'Reilly, M. P., Brown, S. F. and Overy, R. F., Cyclic loading of silty clay with drainage periods, *Journal of Geotechnical Engineering*, ASCE, Vol.117, No.2, 1991, pp.354-362.

Copyright © Int. J. of GEOMATE. All rights reserved, including the making of copies unless permission is obtained from the copyright proprietors.
